Electronic Supplementary Material (ESI) for ChemComm.

SUPPLEMENTARY INFORMATION

1. Materials

1.1. Electrolytic carbon material (ECM)

Electrolytic carbon material was used as the precursor for the synthesis of nanocrystalline diamond. The preparation procedure of ECM is explained as follows: Approximately 250 g of anhydrous LiCl was loaded into a graphite crucible of inner diameter 57 mm and height 130 mm. This was placed in an Inconel retort of inner diameter 125 mm and length 650 mm and heated to a temperature of 770-775 ºC under a flowing atmosphere of dried argon to melt the LiCl, (melting point, 610 ºC). Electrolysis of the molten LiCl was carried out using a 15 mm diameter graphite rod as the cathode with the graphite crucible acting as the anode. Details of the process have been reported elsewhere[1]. Electrolysis was performed with a constant current of 33 A or an initial current density of about 1.0 A cm^{-2} for 1 h.

After electrolysis the cell was allowed to cool to room temperature and the salt removed from the nano-structured carbon material with copious quantities of distilled water. The resulting suspension was vacuum filtered to separate the carbon product and then dried at 100 °C in a vacuum of 0.1 mbar for 6 h, leading to the preparation of about 5 g carbon materials.

1.2. CVD MWCNTs

The structural and thermal behavior of ECM was compared with a commercial CVD MWCNTs purchased from Thomas Swan Advanced Materials (Elicarb®Carbon Nanotubes).

2. Characterization methods

The CVD MWCNTs and ECM samples, in as synthesized and heat treated conditions, were analyzed by a series of techniques. A SDT Q600 analyzer was used for heat treating 2.5 mg

of samples by heating in air to a range of temperatures, followed by quenching in a flow of ambient air. A Philips 1710 high resolution X-ray diffractometer with a Cu anode was used for the phase analysis and a JEOL 6340F field emission scanning electron microscope (SEM) and a JEOL 2000FX analytical transmission electron microscope (TEM) were used for microstructural investigation. The true density was measured using a helium pycnometer of type Micromeritics AccuPyc 1330.

3. XRD characterization

X-ray diffraction measurements were performed on the as-synthesized ECM, heat treated ECM, and CVD-MWCNTs. The XRD patterns obtained are shown in Fig. 1S. It can be seen from Fig. 1S that the (002) graphite reflection in CVD MWCNTs is broader and weaker than that of ECM, which is attributed to the smaller graphitic domains in CVD MWCNTs. Table 1S compiles the XRD data for the hexagonal (002) peaks,i.e., peak position, graphitic layer spacing d002, FWHM as determined by Lorentzian fitting. The table also shows the crystalline domain size L_c as calculated using Scherrer's equation:

$$L_c = (0.9 \times \lambda)/(B \times \cos \Theta) \qquad (1S)$$

where L_c is the average size of the graphitic crystallites, λ is the X-ray wavelength, θ is the Bragg angle, and B is the full peak width at half maximum intensity (FWHM) expressed in radians.

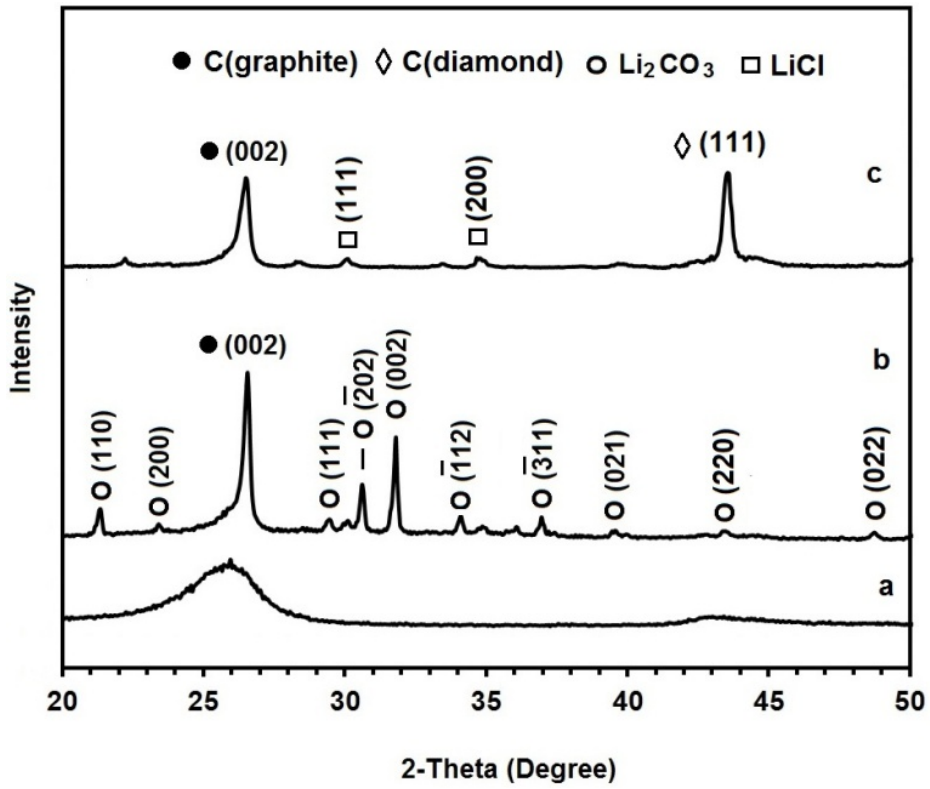

Fig. 1S. XRD patterns of (a) CVD MWCNTs, (b) as-synthesised ECM, and (c) the ECM heated to 515ºC and subsequently cooled down to room temperature under ambient air flow of 100 mL min^{-1}.

Table 1S. XRD data for the hexagonal (002) peaks of the ECM and CVD MWCNTs.

	ECM	CVD MWCNTs
2-theta position (degrees)	26.5502	25.8919
Lattice spacing d_{002} (nm)	3.35735	3.44120
Full width at half maximum (degrees)	0.1968 0.003434808	0.3936 0.006869616
Crystalline domain size L_c (002) (nm)	41.5	20.7

4. Calculation the maximum temperature during the oxidation process

Fig. 4-down panel shows the differential scanning calorimetry (DSC) and thermogravimetry (TG) curves of the ECM heated to 515°C. This figure indicates that the material is oxidized at temperatures between 440°C and 535°C with a peak at 510 °C by heating under ambient air flow of 100 mL min^{-1} under the heating rate of 20 °C min^{-1}. The temperature 515°C is located after the oxidation peak where 57 wt % of the total weight of the material has oxidized.

The heat released upon the oxidation of 57 wt % of the carbon product was calculated from the area under the exothermic peak and found to be Q = 10360 J g^{-1}. In the ideal circumstance, the released heat is consumed for the heating up of the rest of the material from 515°C to a higher temperature. The maximum temperature of the remaining material can be calculated using thermodynamic parameters. The heat capacity of graphite can be expressed by the Eq. (2S) which has been derived based on the data available in the literature[2,3].

$C_p=2\times10^{-10}T^3-1.4\times10^{-6}\times T^2+2.88\times10^{-3}T+1.25\times10^{-1}$ J g^{-1} K^{-1} $T > 560K$ (2S)

where T is in Kelvin and C_p in J K^{-1} g^{-1}.

The melting point and enthalpy of fusion of carbon are ΔH_m = 10 KJ g^{-1} and T_m= 4800 K, respectively[3]. Thermodynamic calculation based on the Eq. (3S) shows that the heat released by burning of 57 wt % the carbon product is enough to reach the temperature of the rest to 4800 K and also causing partial melting.

$$Q \times \frac{57}{43} = \int_{788K}^{4800K} C_p dT + x\Delta H_m \quad (3S)$$

where x is the ratio of the molten carbon in a mixture of solid-liquid.

By substituting the actual parameters into the Eq. (3S), the ratio of the molten carbon, x, can be found to be about 60%.

The above calculation was based on the assumption of adiabatic combustion. In reality, a fraction of the heat generated at the reaction front is dispersed away mainly by the gas products. However, it should be noted that Only 7926 J g^{-1} energy (about 76% of the energy generated in our experiment) is required for increasing the temperature of graphite materials from 788 K to 4800K, according to the Eq.(3S). This means it is very likely that the local temperature of carbon nanomaterials increases to 4800K during the combustion process.

5. Raman analysis of the heat treated carbon product

Raman spectroscopy is widely used in the analysis of sp^2- [4] and sp^3- [5] hybridized carbon-based materials.

The Raman spectrum of the as-synthesized and the heat treated ECM is shown in Fig. 7. The Raman spectrum of the heated product exhibits main features associated with sp^3- and sp^2 - carbon phase, as explained below. A board band is seen in the range of 1300 cm^{-1} - 1380 cm^{-1}. Two well resolved peaks can be distinguished in this band. The peak at 1332 cm^{-1} is the characteristic main first-order lattice vibration of diamond, whereas the peak at 1336 cm^{-1} is assigned to the so-called disorder-induced D line. This peak which usually occurs at about 1360 cm^{-1} [6] refers to the A_{1g} symmetry of sp^2 disordered graphite and indicates the existence of nanocrystalline graphite[7].

However, the position of the D band shifted downward from 1360 cm^{-1} to 1336 cm^{-1}. The downward shift of D peak can be attributed to the presence of sp^3-bonded carbon atoms in the structure of the heat treated material. It has been demonstrated that an increase in sp^3: sp^2 ratio results in a downward shift in the D line[8].

The characteristic peak at 1583 cm^{-1} is G line which is the Raman-active E_{2g} mode corresponding to the movement in the opposite direction of two neighboring carbon atoms in a graphene sheet.

The characteristic peak at 1620 cm^{-1} is assigned to D′ line corresponding to the highest frequency feature in the density of state, which is a defect induced band.

The Raman peaks at 1336, 1583 and 1620 cm^{-1} are characteristic of the presence of nanocrystalline graphite.

As it is obvious from Fig. 7, the intensity of the diamond Raman peak (at 1332 cm^{-1}) is considerably lower than peaks of the nanocrystalline graphite which is due to this fact that visible Raman the excitation line at 633 nm is up to 233 times more sensitive to sp^2 sites than sp^3 sites[9].

In the Raman spectrum of as-synthesized ECM, the peaks of the defect-derived D band, the graphite structure-derived G band, and the defect-induced D′ band appear at 1336 and 1585 and 1620 cm^{-1} respectively.

References

1 A.R. Kamali and D.J. Fray, *Carbon*, 2014, 77, 835.

2 C. Pradere,J.C. Batsale, J.M. Goyheneche, R. Pailler and S. Dilhaire, *Carbon,* 2009, **47**, 737.

3 A.I.Savvatimskiy, *Carbon,*2005, **43**, 1115.

4 M.S.Dresselhaus, A. Jorio and R. Saito, *Annu. Rev. Condens. Matter. Phys.,*2010, **1**, 89.

5 S.Prawer and R.J.Nemanich, *Phil. Trans. R. Soc. A,*2004, **362**, 2537.

6 A.K.M.S.Chowdhury, D.C. Cameron and M.S.J. Hashmi, *Thin Solid Films,* 1998, **332**, 62.

7 G.X.Chen, M.H.Hong andT.C. Chong, *J. Appl. Phys.,* 2004, **95**, 1455.

8 A. Rengan, J.Narayan, C. Jahnke, S.Bedge, J.L. Parkt and M. Li, *Mater.Sci. Eng. B,*1992, **15**, 15.

9 S.R.Sails, D.J. Gardiner, M. Bowden, J. Savage and D. Rodway, *Diamond Relat. Mater.,* 1996, **5**, 589.